Active and passive infrared spectroscopy for the detection of environmental threats

Erik R. Deutsch, Petros Kotidis, Ninghui Zhu, Anish K. Goyal*,
Jim Ye, Alex Mazurenko, Mark Norman, Kostas Zafiriou, Mark Baier, and Ray Connors

Block MEMS/Engineering, 377 Simarano Drive, Marlborough, MA 01752

ABSTRACT

Block MEMS/Engineering develops mid-infrared spectroscopy systems based on both Fourier transform infrared (FTIR) spectrometers and quantum cascade lasers (QCLs). Our recently developed miniaturized external-cavity QCLs are widely tunable over a spectral range of >250 cm^{-1} and tuning can be accomplished at rates of >25 cm^{-1} per millisecond. This enables high-speed mid-infrared spectroscopy of gases and surface contaminants for a variety of military and commercial applications. This paper provides an overview of our FTIR and QCL systems and their defense-related applications.

Keywords: vibrational spectroscopy, infrared spectroscopy, quantum cascade lasers, Fourier-transform infrared (FTIR) spectrometers, chemical detection

1. INTRODUCTION

High sensitivity chemical detection of gases and surface contaminants (both liquids and solids) is readily achieved using mid-infrared (mid-IR) spectroscopy. The mid-IR portion of the optical spectrum spans roughly $\lambda \approx 2.5$ to 14 μm (in wavenumbers, $\bar{\nu} = c/\lambda \approx$ 4000 to 700 cm^{-1}) and mid-IR spectroscopy directly probes the rotational and vibration modes of molecules. The absorption spectra can be rich and the absorption lines can be very strong allowing both high specificity and high sensitivity detection.

Block Engineering has been developing mid-infrared spectroscopy products since 1956 and is, in fact, the originator of the rapid-scan Fourier-Transform Infrared (FTIR) spectrometer. This paper reviews Block Engineering's passive and active mid-IR spectroscopy products and gives examples of their defense-related applications. Particular emphasis is placed on active spectroscopy using the quantum cascade laser (QCL). Block has been leading the miniaturization of the widely tunable QCLs that we believe will enable a wide range of applications.

2. SPECTROSCOPY IN THE MID-INFRARED

This section reviews several factors to consider when performing spectroscopy in the mid-infrared. These include the optical response of chemicals, atmospheric transmission (which is relevant for standoff detection), and thermal background radiation.

Figure 1 plots the mid-IR spectra for the chemical agents VX and HD (sulfur mustard) as well as the explosive material TNT (trinitrotoluene). These show that the mid-IR spectra of chemicals can be rich with many absorption lines to enable highly specific chemical identification. Note also that the absorption lines can be very strong. VX and TNT, for example, both have absorption lines with an absorption depth (where the intensity drops by the factor 1/e) of only ~3 μm. Strong absorption lines enable high sensitivity detection.

* Email: anish.goyal@blockeng.com

Advanced Environmental, Chemical, and Biological Sensing Technologies XI, edited by Tuan Vo-Dinh, Robert A. Lieberman, Günter G. Gauglitz, Proc. of SPIE Vol. 9106, 91060A · © 2014 SPIE · CCC code: 0277-786X/14/$18 · doi: 10.1117/12.2058544

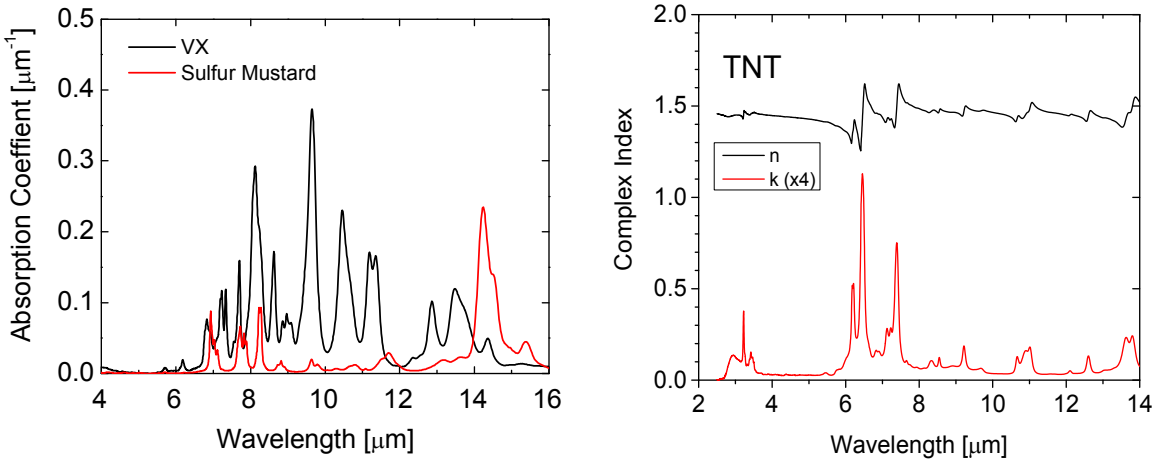

Figure 1: (a) Absorption spectra of the chemical agents VX and sulfur mustard and (b) the complex refractive index of the explosive TNT. Absorption spectra in the mid-IR can be rich with many absorption lines to enable specific chemical identification. Also, the absorption lines can be very strong to enable highly sensitive chemical detection.

The two primary atmospheric transmission windows in the mid-IR are called the mid-wave infrared (MWIR) and long-wave infrared (LWIR). These are shown in Figure 2a to extend roughly between $\lambda \approx 3 - 5$ μm and $\lambda \approx 8 - 14$ μm, respectively. Within the MWIR is a strong CO_2 absorption band at $\lambda = 4.3$ μm. The MWIR is separated from the LWIR by the broad H_2O absorption band centered at $\lambda = 6.3$ μm. Figure 2a plots the effective atmospheric absorption length using $L_{atm} = -R/\ln(T_{atm})$ where T_{atm} is the atmospheric transmittance calculated using HITRAN for a horizontal path at sea level of $R = 10$ meters with a H_2O partial pressure of 7.75×10^{-3} atm. Strictly speaking, the effective absorption length calculated in this way will depend on the choice of R because of the exponential nature of absorption. However, it was found that varying R had only a minor effect on the calculated absorption length. The light gray curve is the high-resolution calculation and the blue curve is obtained by first smoothing the transmittance with a top-hat profile with 5 cm^{-1} bandwidth. As can be seen, the LWIR band is very transparent having absorption lengths of up to ~10 km. Within the H_2O absorption band centered at $\lambda = 6.3$ μm, the smoothed absorption lengths are only on the order of 10 meters. Since the H_2O absorption lines can be very strong, care must be taken to either avoid them or to spectrally average over a sufficiently wide bandwidth.

Over most of the mid-IR, the passive thermal background is greater than the solar irradiance. Figure 2b compares the spectral irradiance from sun [1] with the thermal emission from a blackbody at 300 K. For wavelengths greater than about 5 μm, the blackbody emission exceeds the solar irradiance. For reference, the integrated blackbody emission over the LWIR atmospheric window between $\lambda = 8 - 14$ μm is calculated to be 17.2 mW/cm^2.

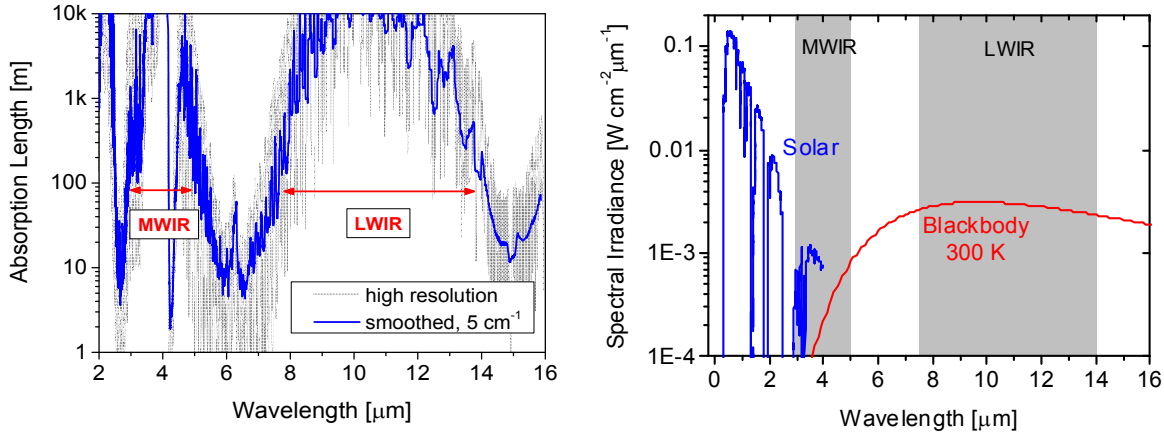

Figure 2: (a) Atmospheric absorption versus wavelength calculated using HITRAN. Results are plotted in terms of the effective absorption length for a horizontal path at sea level. (b) Comparison of spectral irradiance from direct solar illumination and a 300 K blackbody. The MWIR and LWIR atmospheric transmission bands are indicated in both figures.

3. PASSIVE GAS DETECTION USING FTIR SPECTROSCOPY

FTIR spectroscopy is a commonly used method for the detection of gas clouds. Many systems exist to achieve such detection and they can be classified as to whether they use a single element detector or a focal plane array (FPA) for imaging. In either case, a chemical signature is observed when there is a temperature differential between the cloud to be detected and the background. The larger the temperature differential, the larger is the spectral signature of the cloud that is observed using a passive FTIR spectrometer. In this context, the clear sky generally provides excellent spectral signatures while terrestrial backgrounds will provide weaker signatures.

Block builds compact and rugged FTIR systems for passive gas detection. One system called M90 has been used for many years to protect the Pentagon. Another system called PORTHOS™ (PORtable Hazard Observation System) is shown in Figure 3. PORTHOS is a battery-powered, portable FTIR that weighs about 17 pounds. It includes a low-light camera for viewing the scene. The FTIR spectrometer can be configured to have a field of view (FOV) of either 0.5 or 1.5 degrees and the spectral results are analyzed with respect to a built-in chemical library. The battery life is about 4 hours. The system is ideally suited for mobile surveillance by first responders and a tripod-mounted unit can be used for persistent detection. Figure 3 shows an example scenario in which there is an accidental release at a chemical plant. A first responder views the cloud at a standoff distance of up to about 5 km to determine its chemical composition

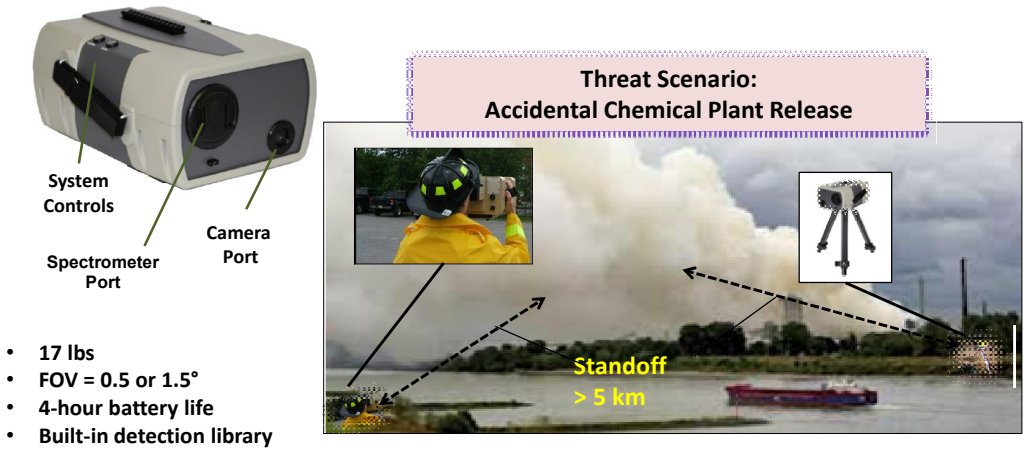

Figure 3: PORTHOS is a passive detection system that incorporates a FTIR spectrometer with detection algorithms and a low-light camera.

4. ACTIVE SPECTROSCOPY USING QUANTUM CASCADE LASERS

QCLs have much higher radiance than thermal sources to allow the projection of optical power over long distances. Blackbody thermal sources called "globars" are often used in conjunction with FTIR spectrometers for micro-spectroscopy in the mid-IR [2]. A thermal source at 1100 K has a radiance of 0.3 W/cm^2/sr over the $\lambda = 8 - 14$ μm band. In comparison, a 1-mW diffraction-limited laser beam at $\lambda = 10$ μm has a radiance of about 10^3 W/cm^2/sr which is roughly 10^4 greater than for the thermal source. Although thermal sources have been used with FTIR spectrometers for standoff surface detection, these are not viable for longer ranges [3, 4].

QCLs are a revolutionary mid-IR laser technology that makes mid-IR spectroscopy practical in configurations that were previously not possible [5]. Prior to the invention of QCLs in 1994 [6], wavelength-tunable mid-IR sources included lead-salt lasers [7], antimonide-based lasers [8], carbon-dioxide lasers [9], synchrotron radiation [10], and optical parametric oscillators [11-13]. QCLs will largely supplant these other technologies for mid-IR spectroscopy applications because they can provide continuous wavelength coverage over much of the mid-IR (at least $\lambda > 3 - 14$ μm) with high power and excellent beam quality. Furthermore, they operate at room temperature and are compact, efficient, and reliable [14].

Much progress has been made to increase the gain bandwidth from a single laser chip [15, 16]. Wavelength tuning in QCLs is typically achieved by placing the QCL chip in an external cavity that incorporates a dispersive element such as a diffraction grating. In such external-cavity QCLs (EC-QCLs), the wavelength is tuned over the gain bandwidth of the laser chip by rotating the grating or mirror within the cavity. Therefore, this approach involves mechanical motion of optical components which will ultimately limit the tuning speed. The widest tuning that has been reported to date from a single laser chip is $\lambda = 7.6 - 11.4$ μm ($\Delta\nu = 432$ cm^{-1}) [15]. Alternative approaches to wavelength tuning that do not involve an external cavity are an area of active research [17-23].

4.1 EC-QCLs from Block MEMS/Engineering

Block MEMS/Engineering is leading the development of miniaturized, widely tunable EC-QCLs. Figure 4 shows a schematic of the optical configuration of an EC-QCL. The laser cavity is formed between the front facet of a QCL chip and a diffraction grating. The laser facet that faces the diffraction grating is anti-reflection coated. A pair of lenses collimates the highly divergent emission from the QCL chip and the diffraction grating selects the emission wavelength. Block has packaged the EC-QCL within a module called the Mini-QCL™ which has dimensions (excluding the electrical leads) of only 43 x 23 x 17 mm (L x W x H). Currently, modules are available that operate within the $\lambda = 5.4 - 13.3$ μm range with each module being able to tune over >250 cm^{-1}. Lasers operate pulsed with peak powers of 100's

of mW. The beams have near-diffraction-limited beam quality and the beam pointing stability is excellent. To the best of our knowledge, these modules have the fastest available tuning speeds of at least 25 cm^{-1}/msec of any widely tunable EC-QCL. This enables tuning over a bandwidth of >250 cm^{-1} at scan rates >100 Hz.

Up to four (4) Mini-QCL modules can be incorporated into a fully integrated LaserTune™ system that includes all of the necessary electronics to drive the lasers. A single LaserTune system can have a gap-free tuning range of λ = 5.3 – 13.3 μm. By "gap-free" is meant that the tuning is continuous with no gaps in wavelength. Figure 4 shows an example tuning curve for operation with 50-ns-long pulses at 5% duty factor. Furthermore, the system is designed to be able to perform spectroscopy when an external detector is attached. Depending on how the laser and detector are configured, the system can be used, for example, to perform spectroscopy in transmission mode with a gas cell or in reflection mode for detecting contaminants on surfaces.

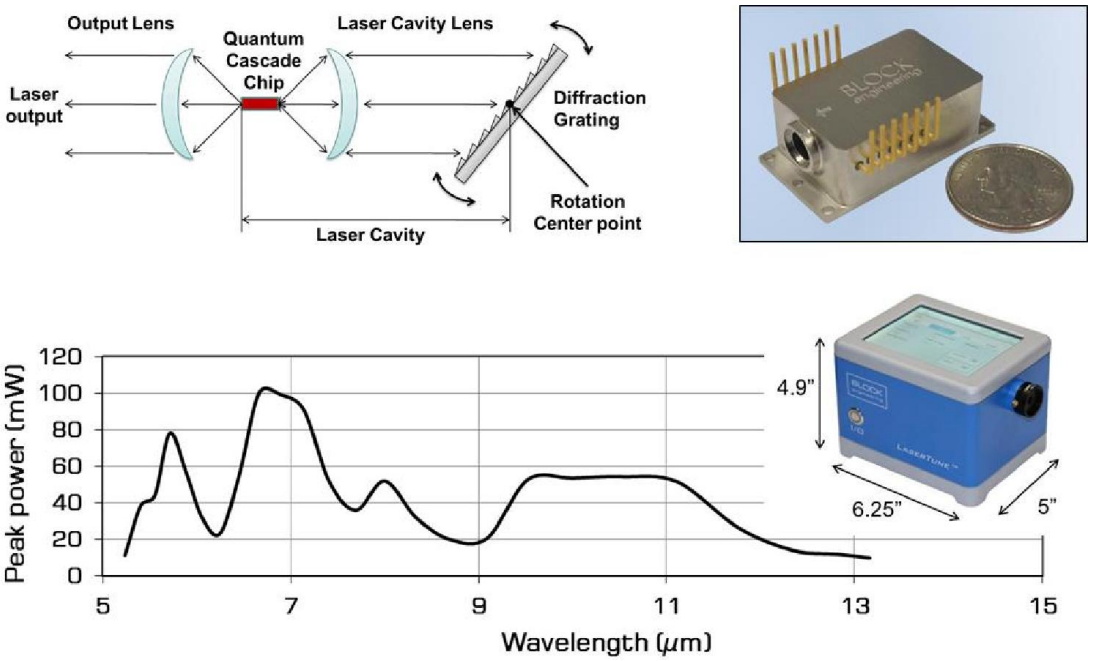

Figure 4: (Top left) Schematic diagram of an external-cavity QCL. (Top right) Photograph of a Mini-QCL which is the smallest widely tunable EC-QCL to the best of our knowledge. (Bottom) Photograph of LaserTune which is a fully integrated laser system including electronics. Also shown is an example tuning curve for a LaserTune system operating with 50-ns-long pulses at 5% duty factor. The gap-free tuning range for this system is λ = 5.4 – 13.3 μm.

4.2 Application to gas sensing

Figure 5 shows data taken using an older version of the LaserTune at the Edgewood Chemical and Biological Center (ECBC) for the detection of chemical agents in vapor form. As shown in the photograph, the LaserTune was coupled to a 10-meter gas cell and the transmitted light was detected using a thermoelectrically cooled (TEC) mercury cadmium telluride (MCT) detector. The spectral absorbance of the chemical agents GB (sarin), GD (soman), and HD (sulfur mustard), were measured versus concentration. These measurements yielded limits of quantification of a few mg/m^3. With improvements to the system, we calculate that the limits of detection (LOD) can be improved by a factor of 100 – 1000x as compared to these early results.

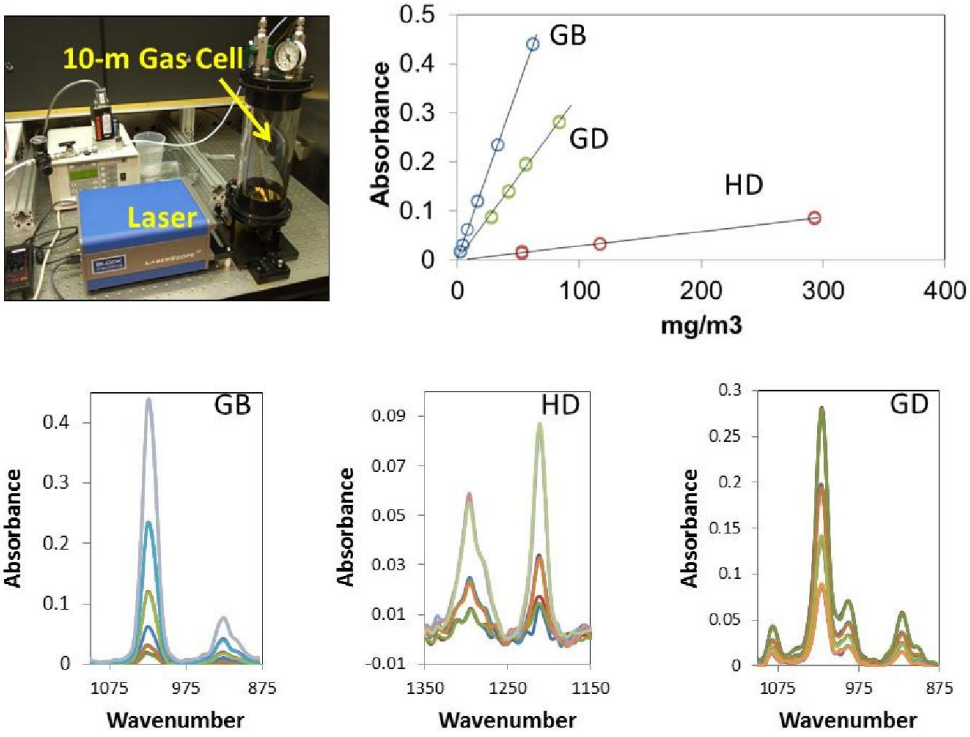

Figure 5: Transmission measurements of chemical agents in a 10-m-long gas cell were made at ECBC using the LaserTune with an associated MCT detector.

Since the QCLs have nearly diffraction-limited beam profiles, the laser beams can propagate over long distances with minimal divergence. Therefore, it is possible to perform line-of-sight gas detection over long distances. Figure 6 shows a system concept called LaserWarn™ for protection of facilities. A LaserWarn transceiver includes the laser, detector, and associated optics. The transceiver is sequentially pointed towards low-cost retroreflectors that are placed at opposite ends of the facility and measures the transmittance along each of the beam paths. Collectively, these beam paths form an "optical fence" around the facility. If a threat cloud crosses the "optical fence" then its presence will be detected by the system. Rather than sequentially interrogating multiple beam paths, it is also possible to configure a system of mirrors such that the laser beam crisscrosses the facility in such a way that the transceiver does not need to move. The LaserWarn system is also applicable to the protection of large indoor areas such as airports. Advantages of this approach include the ability to detect a wide range of gases with high sensitivity over large distances (several kilometers). Also, the system requires no consumables and results in low maintenance compared to a network of point sensors.

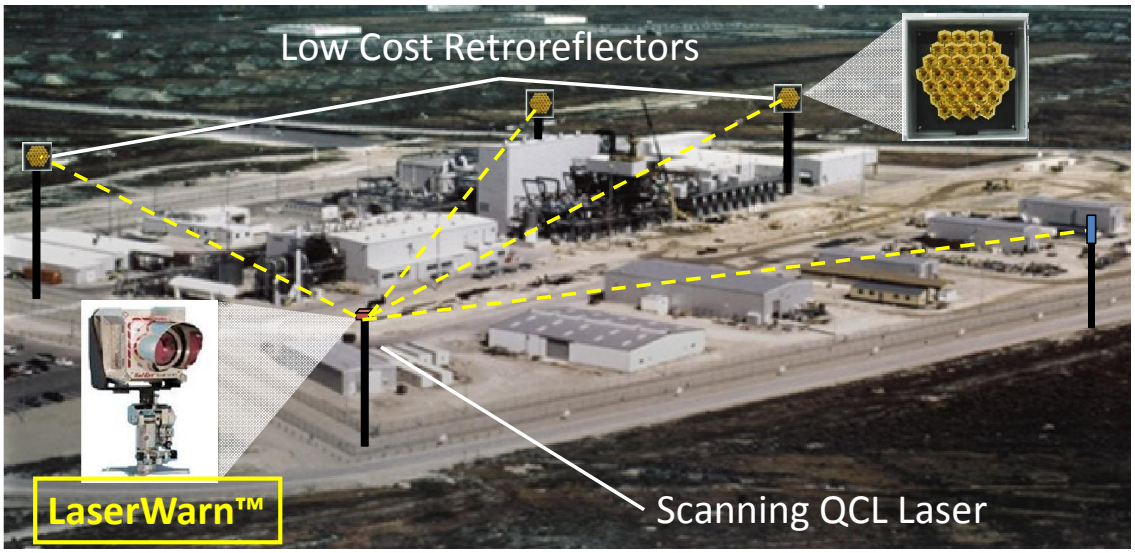

Figure 6: LaserWarn system for the protection of facilities. The LaserWarn transceiver includes a laser, detector, and associated optics. When used in conjunction with retroreflectors and mirrors, it forms an "optical fence" that alarms when a threat cloud crosses its boundary. This figure shows an example of an outdoor system. The system can also be used to protect large indoor facilities.

4.3 Application to surface sensing

Mid-IR spectroscopy is a powerful method for the identification of bulk materials as well as trace contaminants on surfaces. For surface sensing, Block has developed the LaserScan™ system which, as shown in Figure 7, incorporates a widely tunable EC-QCL source and an infrared detector. The system measures the spectral reflectance from a surface that is typically 150 mm away from the instrument. It is designed to measure a wide range of surface that range from being diffusely reflecting to specularly reflecting. And since the laser beams have relatively low average power, the system is eye safe. We have developed both a handheld unit for field use and a fixed unit for use in process-control applications.

Figure 8 shows the spectral reflectance of a variety of plastics made using the LaserScan. Figure 9 shows the spectral reflectance of both liquid and surface contaminants. Figure 9a shows the reflectance of methyl ethyl salicylate (MES) on linoleum and compares with the library spectrum. The rich absorption spectrum clearly enables high specificity detection. Figure 9b shows the measured reflectance of trace levels of the explosive RDX on painted metal (concentration unknown). These are compared with the reference spectrum which again clearly demonstrates the ability of mid-IR reflectance spectroscopy to detect chemical contamination on surfaces.

Figure 10 plots the calculated reflectance from a film of silicone oil on either a reflective metal surface or a dielectric. Silicone is used here as an example chemical contaminant. For a 1-μm-thick film on metal, the reflectance spectrum has minima at the absorption lines of silicone oil. For a 1-μm-thick film on a dielectric substrate with refractive index of 1.5, the reflectance spectrum is inverted in that the reflection spectrum has maxima near the locations of the absorption lines. This demonstrates that the reflection spectrum from a contaminated surface is strongly affected by the properties of the underlying substrate. Nevertheless, calculations indicate that silicone can be detected on either type of substrate at concentrations of only a few $\mu g/cm^2$. This shows the high sensitivity of mid-IR spectroscopy.

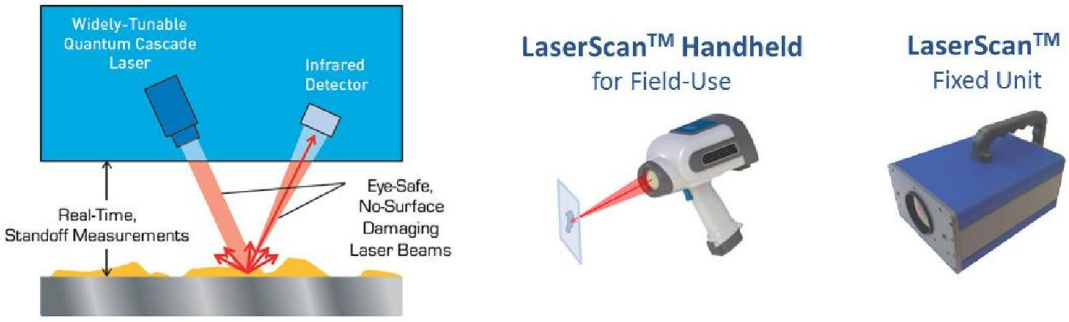

Figure 7: LaserScan system for measuring the spectral reflectance from surfaces for the identification of bulk materials or trace contaminants. The system is available in both handheld and fixed units.

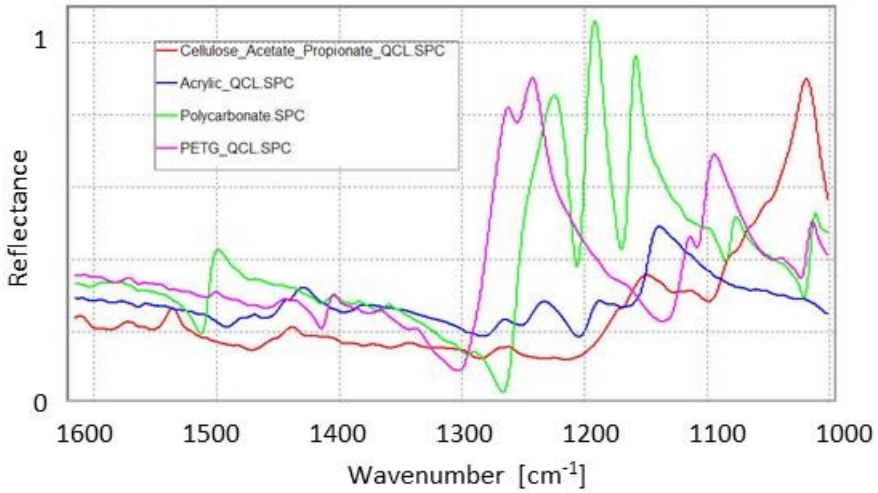

Figure 8: Differentiation of various plastics using the LaserScan including cellulose acetate, acrylic, polycarbonate, and polyethylene.

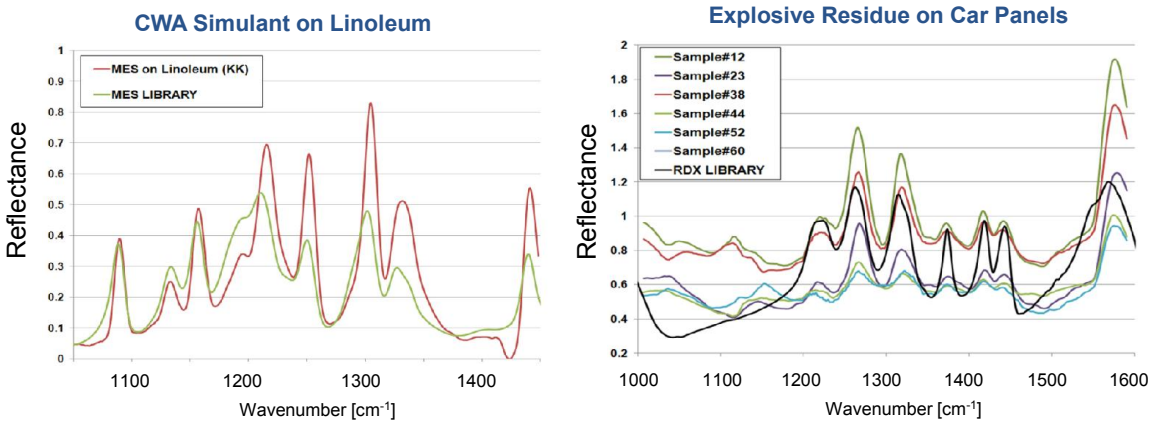

Figure 9: (a) Reflection spectrum of methyl ethyl salicylate (MES) on linoleum and (b) RDX residue on painted metal. The measured spectra compare favorably with the library spectra.

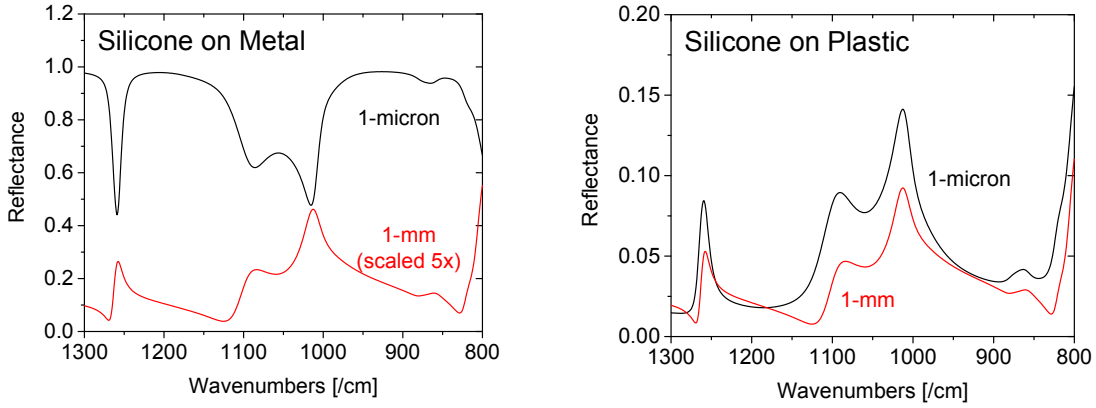

Figure 10: Calculated reflectance of a film of silicone oil on either (a) reflective metal surface or (b) dielectric with refractive index of 1.5. For silicone on the metallic surface, the reflectance spectrum has minima where the silicone oil is absorbing. For silicone oil on the dielectric, the spectrum is inverted. Detection limits are only a few μg/cm^2.

Figure 11 shows initial work on the imaging of explosive residue on surfaces. Here a residue of TNT is applied to a surface. When the laser is tuned to an absorption line of the TNT at 1355 cm^{-1}, the presence of the TNT is clearly observed in the difference image. When the laser is tuned to a wavelength where the TNT is not absorbing at 1079 cm^{-1}, the reflectance is not affected and the difference image does not highlight the presence of the TNT. Future work will involve generating hyperspectral images for the detection and mapping of surface contaminants.

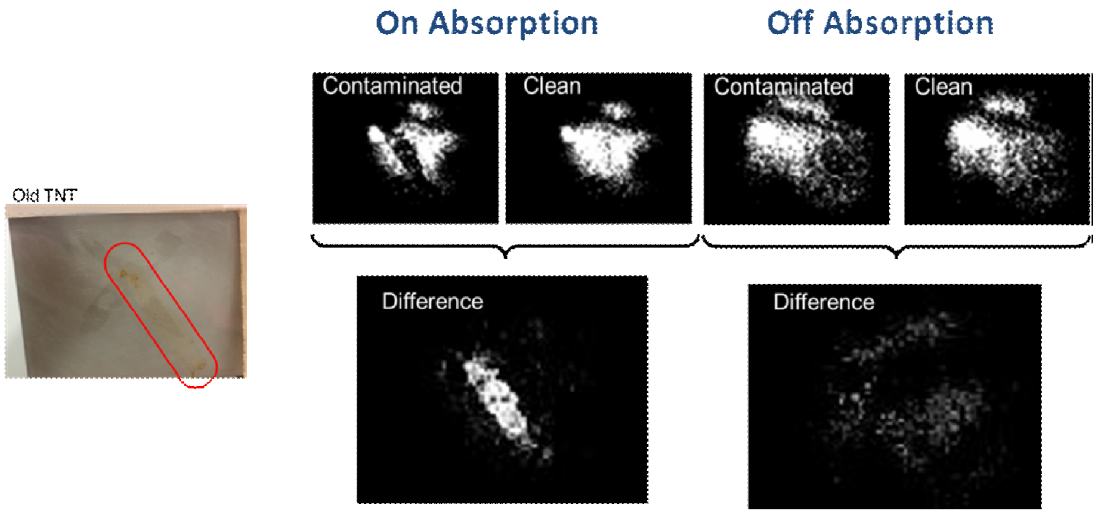

Figure 11: Imaging of TNT residue on a surface by measuring the reflectance when the laser is tuned on and off of an absorption line of TNT.

5. SUMMARY

Block MEMS/Engineering has a long history of developing mid-IR spectroscopy products. This includes FTIR spectrometers and more recently miniaturized widely tunable QCLs. These have application to the high sensitivity detection of gases and surface contaminants.

Acknowledgements: The authors gratefully acknowledge the contributions and support of Daniel Cavicchio, John Coates, Scott Riggi, and Plamen Krastev.

REFERENCES

1. ASTM G173-03(2012) Standard tables for reference solar spectral irradiances.
2. R. Bhargava, "Infrared spectroscopic imaging: The next generation," Applied Spectroscopy **66**, 1091-1120 (2012).
3. R. Harig, R. Braun, C. Dyer, C. Howle, and B. Truscott, "Short-range remote detection of liquid surface contamination by active imaging Fourier transform spectrometry," Opt. Express **16**, 5708-5714 (2008).
4. L. Pacheco-Londoño, W. Ortiz-Rivera, O. Primera-Pedrozo, and S. Hernández-Rivera, "Vibrational spectroscopy standoff detection of explosives," Analytical and Bioanalytical Chemistry **395**, 323-335 (2009).
5. C. K. N. Patel, A. Lyakh, R. Maulini, A. Tsekoun, and B. Tadjikov, "QCL as a game changer in MWIR and LWIR military and homeland security applications," Proc. SPIE **8373**, 83732E (2012).
6. J. Faist, F. Capasso, D. Sivco, C. Sirtori, A. L. Hutchinson, and A. Cho, "Quantum cascade laser," Science **264**, 553-556 (1994).
7. M. Tacke, "Lead-salt lasers," Philosophical Transactions of the Royal Society A **359**, 547-566 (2001).
8. L. J. Olafsen, "Antimonide Mid-IR Lasers," in *Long-Wavelength Infrared Semiconductor Lasers*, H. K. Choi, ed. (John Wiley and Sons, 2004).
9. A. Bell, C. Dyer, A. W. Jones, and K. Kinnear, "Standoff liquid CW detection," Proc. SPIE **5268**, 302-309 (2004).
10. C. R. Liao, M. Rak, J. Lund, M. Unger, E. Platt, B. C. Albensi, C. J. Hirschmugl, and K. M. Gough, "Synchrotron FTIR reveals lipid around and within amyloid plaques in transgenic mice and Alzheimer's disease brain," Analyst **138**, 3991-3997 (2013).
11. C. R. Howle, D. J. M. Stothard, C. F. Rae, M. Ross, B. S. Truscott, C. D. Dyer, and M. H. Dunn, "Active hyperspectral imaging system for the detection of liquids," Proc. SPIE **6954**, 69540L (2008).
12. E. Lippert, H. Fonnum, G. Arisholm, and K. Stenersen, "A 22-watt mid-infrared optical parametric oscillator with V-shaped 3-mirror ring resonator," Optics Express **18**, 26475-26483 (2010).
13. C. R. Swim, "Review of active chem-bio sensing," Proc. SPIE **5416**, 178-185 (2004).
14. J. Faist, *Quantum Cascade Laser* (Oxford University Press, 2013).
15. A. Hugi, R. Terazzi, Y. Bonetti, A. Wittmann, M. Fischer, M. Beck, J. Faist, and E. Gini, "External cavity quantum cascade laser tunable from 7.6 to 11.4 μm," Appl. Phys. Lett. **95**, 061103-061103 (2009).
16. T. Dougakiuchi, M. Fujita, N. Akikusa, A. Sugiyama, T. Edamura, and M. Yamanishi, "Broadband tuning of external-cavity dual-upper-state quantum-cascade lasers in continuous wave operation," Applied Physics Express **4**, 102101 (2011).
17. T. S. Mansuripur, S. Menzel, R. Blanchard, L. Diehl, C. Pflugl, Y. Huang, J.-H. Ryou, R. D. Dupuis, M. Loncar, and F. Capasso, "Widely tunable mid-infrared quantum cascade lasers using sampled grating reflectors," Optics Express **20**, 23339-23348 (2012).
18. P. Fuchs, J. Seufert, J. Koeth, J. Semmel, S. Hofling, L. Worschech, and A. Forchel, "Widely tunable quantum cascade lasers with coupled cavities for gas detection," Appl. Phys. Lett. **97**, 181111 (2010).
19. B. G. Lee, H. A. Zhang, C. Pflugl, L. Diehl, M. A. Belkin, M. Fischer, A. Wittmann, J. Faist, and F. Capasso, "Broadband distributed-feedback quantum cascade laser array operating from 8.0 to 9.8 mm," IEEE Photonics Technology Letters **21**, 914-916 (2009).
20. P. Rauter, S. Menzel, A. K. Goyal, C. A. Wang, A. Sanchez, G. Turner, and F. Capasso, "High-power arrays of quantum cascade laser master-oscillator power-amplifiers," Optics Express **21**, 4518-4530 (2013).
21. P. Rauter, S. Menzel, B. Gokden, A. K. Goyal, C. A. Wang, A. Sanchez, G. Turner, and F. Capasso, "Single-mode tapered quantum cascade lasers," Appl. Phys. Lett. **102**, 181102 (2013).
22. A. K. Goyal, M. Spencer, O. Shatrovoy, B. G. Lee, L. Diehl, C. Pfluegl, A. Sanchez, and F. Capasso, "Dispersion-compensated wavelength beam combining of quantum-cascade-laser arrays," Optics Express **19**, 26725-26732 (2011).
23. A. K. Goyal, T. Myers, C. A. Wang, M. Kelly, B. Tyrrell, B. Gokden, A. Sanchez, G. Turner, and F. Capasso, "Active hyperspectral imaging using a quantum cascade laser (QCL) array and a digital-pixel focal plane array (DFPA) camera," Optics Express, (submitted) (2014).